

# Structured Sparse Non-negative Matrix Factorization with $\ell_{2,0}$ -Norm for scRNA-seq Data Analysis

Wenwen Min, Taosheng Xu, Xiang Wan and Tsung-Hui Chang

**Abstract**—Non-negative matrix factorization (NMF) is a powerful tool for dimensionality reduction and clustering. Unfortunately, the interpretation of the clustering results from NMF is difficult, especially for the high-dimensional biological data without effective feature selection. In this paper, we first introduce a row-sparse NMF with  $\ell_{2,0}$ -norm constraint (NMF- $\ell_{20}$ ), where the basis matrix  $W$  is constrained by the  $\ell_{2,0}$ -norm, such that  $W$  has a row-sparsity pattern with feature selection. It is a challenge to solve the model, because the  $\ell_{2,0}$ -norm is non-convex and non-smooth. Fortunately, we prove that the  $\ell_{2,0}$ -norm satisfies the Kurdyka-Łojasiewicz property. Based on the finding, we present a proximal alternating linearized minimization algorithm and its monotone accelerated version to solve the NMF- $\ell_{20}$  model. In addition, we also present a orthogonal NMF with  $\ell_{2,0}$ -norm constraint (ONMF- $\ell_{20}$ ) to enhance the clustering performance by using a non-negative orthogonal constraint. We propose an efficient algorithm to solve ONMF- $\ell_{20}$  by transforming it into a series of constrained and penalized matrix factorization problems. The results on numerical and scRNA-seq datasets demonstrate the efficiency of our methods in comparison with existing methods.

**Index Terms**— $\ell_{2,0}$ -norm, feature selection, row sparse NMF and ONMF, non-convex optimization, scRNA-seq data clustering

## I. INTRODUCTION

WITH the development of single cell RNA sequencing (scRNA-seq) technology, we can easily obtain biological profile data at single cell level from thousands of cells at the same time [1]. Clustering such scRNA-seq data has been becoming increasingly important for biological and medical applications [2].

Non-negative matrix factorization (NMF) and its variants have been widely used to solve some computational biological problems [3–9]. Especially, they have achieved lots of successfully applications in scRNA-seq data clustering analysis [10–12]. However, the NMF class algorithms expose some shortcomings when being applied to the clustering analysis of the high-dimensional biological data. It is well known that

the high-dimensional biological data contains many noisy and redundant features which often impacts the performance of clustering algorithms.

To overcome the problems, sparse NMF methods have been proposed by adding sparseness constraints [13–15]. At present, the proposed sparseness constraints, such as  $\ell_1$  and  $\ell_0$  norms, cannot identify real row-sparsity patterns of the basis matrix  $W$  in NMF,  $X \approx WH$  (see Figure 1A and B), such that these sparse NMF methods cannot select the important features for clustering analysis.

Feature selection is a effective way that extract the informative features to improve the interpretability and performance of machine learning models [16, 17]. To enhance model interpretability, a common task is to search for some most important information features when NMF and its variants are used for high-dimensional data analysis. Previously,  $\ell_{2,1}$ -norm constraint has been used in some supervised learning models to perform feature selection [17, 18]. Moreover,  $\ell_{2,0}$ -norm is more desirable from the sparsity perspective, because it can select a specific number of the important information features [19–21].

To integrate feature selection in the NMF model, we first present a row-sparse NMF with  $\ell_{2,0}$ -norm constraint (NMF- $\ell_{20}$ ). The basis matrix  $W$  is constrained by the  $\ell_{2,0}$ -norm, such that  $W$  has a row-sparsity pattern with feature selection (see Figure 1C). However, it is difficult to find an effective convergence algorithm to solve the NMF- $\ell_{20}$  model because the  $\ell_{2,0}$ -norm constraint is non-convex and non-smooth. Fortunately, we find that the  $\ell_{2,0}$ -norm satisfies the Kurdyka-Łojasiewicz (KŁ) property such that the traditional proximal gradient method can be used to solve a class of optimization problems with  $\ell_{2,0}$ -norm constraint. For instance, the proximal alternating linearized minimization (PALM) algorithm has been proposed to solve a class of non-convex and non-smooth problems which satisfy KŁ property [22]. Based on the above point, we introduce the PALM algorithm and its variant, a monotone accelerated PALM (maPALM) algorithm, to solve the NMF- $\ell_{2,0}$  model. We prove that both PALM and maPALM algorithms converge to a critical point when they are used to solve the NMF- $\ell_{20}$  model.

In addition, we also note that the orthogonal NMF (ONMF) which is a variant of NMF. It improves the clustering performance by adding the non-negative orthogonal constraint [23–25]. Non-negative orthogonal matrix has the following two properties: (1) an orthonormal matrix forms a basis for a specific subspace, which facilitates geometric interpretation and signal reconstruction; (2) two non-negative vectors in the matrix are orthogonal if and only if their nonzero dimensions

Wenwen Min is with The Chinese University of Hong Kong, Shenzhen 518172, China, University of Science and Technology of China, Hefei 230027, China, and the Shenzhen Research Institute of Big Data, Shenzhen 518172, China. E-mail: minwenwen@ustc.edu.cn.

Taosheng Xu is with Warshel Institute for Computational Biology, The Chinese University of Hong Kong, Shenzhen 518172, China, University of Science and Technology of China, Hefei 230027, China. E-mail: taosheng.x@gmail.com

Xiang Wan is with the Shenzhen Research Institute of Big Data, Shenzhen 518172, China. E-mail: wanxiang@sribd.cn.

Tsung-Hui Chang is with The Chinese University of Hong Kong, Shenzhen 518172, China and the Shenzhen Research Institute of Big Data, Shenzhen 518172, China. E-mail: tsunghui.chang@ieee.org.

Manuscript received XX, 2021; revised XX, 2021.

do not overlap. This may be the reason why ONMF is sometime more effective than NMF in clustering.

To integrate feature selection and non-negative orthogonal constraint in the NMF model, we also present a row-sparse ONMF with  $\ell_{2,0}$ -norm constraint (ONMF- $\ell_{20}$ ). We propose an efficient algorithm for ONMF- $\ell_{20}$  model by using a penalty function method. The algorithm transforms ONMF- $\ell_{20}$  into a series of subproblems so that the PALM and maPALM algorithms can be used to solve them. Our contributions of this paper are summarized as follows:

- 1) We prove that the  $\ell_{2,0}$ -norm satisfies the KL property such that a class of optimization problems with  $\ell_{2,0}$ -norm constraint can be solved by the PALM algorithm.
- 2) An efficient algorithm (PALM) for NMF- $\ell_{20}$ , and its convergence property.
- 3) An accelerated version of PALM (maPALM) for NMF- $\ell_{20}$ , and its convergence property.
- 4) An efficient algorithm for ONMF- $\ell_{20}$  by transforming it into a series of subproblems, and its convergence property.
- 5) The application of our methods and the comparison with the competing methods using the simulated and scRNA-seq datasets. The results show that our methods are more effective in clustering accuracy and feature selection.

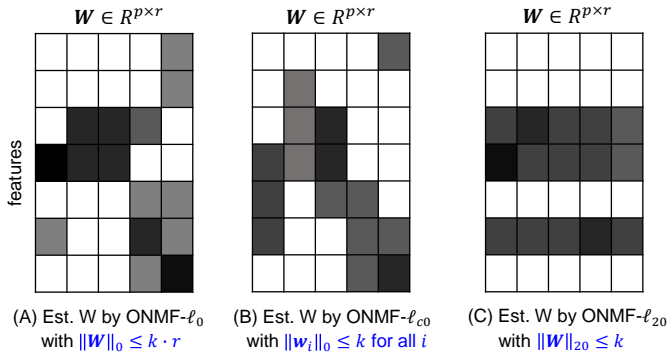


Figure 1. Illustration of these basis matrices  $\mathbf{W}$  obtained from three structured sparse NMF models ( $\mathbf{X} \approx \mathbf{W}\mathbf{H}$ ) with different constraints. (A) showing estimated  $\mathbf{W}$  by NMF- $\ell_0$ , (B) showing estimated  $\mathbf{W}$  by NMF- $\ell_{20}$ , and (C) showing estimated  $\mathbf{W}$  by NMF- $\ell_{c0}$ , where dark boxes denote the non-zero coefficients and blank boxes represent zero coefficients. The constraint conditions of  $\mathbf{W}$  in NMF- $\ell_0$ , NMF- $\ell_{20}$  and NMF- $\ell_{c0}$  are defined in Table I.

## II. NOTATIONS AND DEFINITIONS

Given a matrix  $\mathbf{W} \in \mathbb{R}^{p \times r}$ , let  $\mathbf{w}^i$  and  $\mathbf{w}_j$  denote its  $i$ -th row and  $j$ -th column, respectively. The Frobenius norm of  $\mathbf{W} \in \mathbb{R}^{p \times n}$  is defined as:

$$\|\mathbf{W}\|_F = \sqrt{\sum_{i=1}^p \sum_{j=1}^r w_{ij}^2} = \sqrt{\text{tr}(\mathbf{W}^T \mathbf{W})}. \quad (1)$$

The spectral norm of  $\mathbf{W}$  is the largest singular value of  $\mathbf{W}$  and it is defined as:

$$\|\mathbf{W}\|_2 = \sigma_{\max}(\mathbf{W}), \quad (2)$$

Table I  
SUMMARY OF NOTATIONS.

Notation	Meaning
Normal font, e.g., $x$	A scalar
Bold lowercase, e.g., $\mathbf{w}$	A vector
Bold capital, e.g., $\mathbf{W}$	A matrix
$\mathbf{X}$	A $p$ -by- $n$ matrix
$\mathbf{W}$	A $p$ -by- $r$ matrix
$\mathbf{H}$	An $r$ -by- $n$ matrix
$\mathbf{I}_r$	An $r \times r$ identity matrix
$\mathbf{h}^i$	The $i$ -th row of $\mathbf{H}$
$\mathbf{h}_j$	The $j$ -th column of $\mathbf{H}$
$\ \cdot\ _1$	$\ell_1$ -norm for a vector
$\ \cdot\ _0$	$\ell_0$ -norm for a vector
$\ \cdot\ _2$ or $\ \cdot\ $	$\ell_2$ -norm for a vector
$\ \cdot\ _F$	Frobenius norm for a matrix
$\ \cdot\ _2$	Spectral norm for a matrix
$I(\cdot)$	Indicator function
Model	Constraint condition
NMF- $\ell_0$	$\ \mathbf{W}\ _0 \leq k \cdot r$ (see Eq. 3)
NMF- $\ell_{20}$	$\ \mathbf{W}\ _{2,0} \leq k$ (see Eq. 4)
NMF- $\ell_{c0}$	Column-wise sparsity of $\mathbf{W}$ (see Eq. 8)

The  $\ell_0$ -norm of  $\mathbf{W}$  is defined as:

$$\|\mathbf{W}\|_0 = \sum_{i=1}^p \sum_{j=1}^n I(w_{ij} \neq 0) = \sum_{i=1}^p \|\mathbf{w}^i\|_0 = \sum_{j=1}^r \|\mathbf{w}_j\|_0, \quad (3)$$

where  $I(x) = 1$  if  $x \neq 0$ ,  $I(x) = 0$  if  $x = 0$ . The  $\ell_{2,0}$ -norm of  $\mathbf{W}$  is defined as:

$$\|\mathbf{W}\|_{2,0} = \sum_{i=1}^p I(\|\mathbf{w}^i\| \neq 0) = \|\|\mathbf{w}^1\|, \dots, \|\mathbf{w}^p\|\|_0, \quad (4)$$

where  $\|\cdot\|$  is the  $\ell_2$ -norm and  $\|\mathbf{x}\| = \sum x_i^2$ . Briefly,  $\|\mathbf{W}\|_{2,0}$  denotes the number of non-zero rows in  $\mathbf{W}$ . More notations are summarized in Table I and the mathematical definitions for nonconvex optimization are summarized into the appendix A-A. For simplicity,  $\ell_{2,0}$  and  $\|\mathbf{W}\|_{2,0}$  sometimes are abbreviated as  $\ell_{20}$  and  $\|\mathbf{W}\|_{20}$ , respectively.

## III. PROPOSED FRAMEWORK

### A. NMF and ONMF

Given a data  $\mathbf{X} \in \mathbb{R}^{p \times n}$  with  $p$  features and  $n$  samples, NMF model [26] can be written as follows:

$$\begin{aligned} & \underset{\mathbf{W}, \mathbf{H}}{\text{minimize}} && \|\mathbf{X} - \mathbf{W}\mathbf{H}\|_F^2 \\ & \text{subject to} && \mathbf{W} \in \mathbb{R}_+^{p \times r}, \mathbf{H} \in \mathbb{R}_+^{r \times n}. \end{aligned} \quad (5)$$

[23] has reported that ONMF can improve the clustering performance by adding the non-negative orthogonal constraint on  $\mathbf{H}$ . Thus, we introduce the following ONMF model:

$$\begin{aligned} & \underset{\mathbf{W}, \mathbf{H}}{\text{minimize}} && \|\mathbf{X} - \mathbf{W}\mathbf{H}\|_F^2 \\ & \text{subject to} && \mathbf{W} \in \mathbb{R}_+^{p \times r}, \mathbf{H} \in \mathbb{R}_+^{r \times n}, \mathbf{H}\mathbf{H}^T = \mathbf{I}_r. \end{aligned} \quad (6)$$

Theorem 1 in reference [23] has shown that ONMF is equivalent to k-means clustering, because the nonnegative orthogonal matrix  $\mathbf{H}$  has a good property (see remark 1).

*Remark 1.* For the solution  $\mathbf{H}$  of Eq. (6), it has at most one non-zero entry in each column, because  $\mathbf{H}$  is non-negative and satisfies orthogonality  $\mathbf{H}\mathbf{H}^T = \mathbf{I}_r$ .

### B. Structured sparse NMF (SSNMF)

To integrate feature selection and non-negative orthogonal constraint in NMF model, we introduce a row-sparse ONMF with  $\ell_{2,0}$ -norm constraint (ONMF- $\ell_{20}$ ):

$$\begin{aligned} & \underset{\mathbf{W}, \mathbf{H}}{\text{minimize}} && \|\mathbf{X} - \mathbf{W}\mathbf{H}\|_F^2 \\ & \text{subject to} && \mathbf{W} \in \Omega_w := \{\mathbf{W} \in \mathbb{R}_+^{p \times r} : \|\mathbf{W}\|_{2,0} \leq k\}, \\ & && \mathbf{H} \in \Omega_h := \{\mathbf{H} \in \mathbb{R}_+^{r \times n} : \mathbf{H}\mathbf{H}^T = \mathbf{I}_r\}, \end{aligned} \quad (7)$$

where  $\|\mathbf{W}\|_{2,0} \leq k$  encourages  $\mathbf{W}$  to be row sparse and select some most important features. We can also make  $\mathbf{W}$  column sparse using the following constraint, named  $\ell_{c0}$ -norm, which uses  $\ell_0$ -norm to each column of  $\mathbf{W}$ :

$$\Omega_w := \{\mathbf{W} \in \mathbb{R}_+^{p \times r} : \|\mathbf{w}_j\|_0 \leq s, \forall j\}. \quad (8)$$

The key to solve problem (7) is to remove its orthogonal constraint. Based on the conclusion of Eq. (8) from reference [25], Eq. (7) is equivalent to:

$$\begin{aligned} & \underset{\mathbf{W}, \mathbf{H}}{\text{minimize}} && \|\mathbf{X} - \mathbf{W}\mathbf{H}\|_F^2 \\ & \text{subject to} && \mathbf{W} \in \Omega_w := \{\mathbf{W} \in \mathbb{R}_+^{p \times r} : \|\mathbf{W}\|_{2,0} \leq k\}, \\ & && \mathbf{H} \in \{\mathbf{H} \in \mathbb{R}_+^{r \times n} : \|\mathbf{h}_j\|_1^2 = \|\mathbf{h}_j\|_2^2, \forall j\}. \end{aligned} \quad (9)$$

We consider its penalized formulation and present a SSNMF framework as follows:

$$\begin{aligned} & \underset{\mathbf{W}, \mathbf{H}}{\text{minimize}} && \frac{1}{2} \|\mathbf{X} - \mathbf{W}\mathbf{H}\|_F^2 + \frac{\rho}{2} \sum_{j=1}^n \left( (1^T \mathbf{h}_j)^2 - \|\mathbf{h}_j\|_2^2 \right) \\ & \text{subject to} && \mathbf{W} \in \Omega_w := \{\mathbf{W} \in \mathbb{R}_+^{p \times r} : \|\mathbf{W}\|_{2,0} \leq k\}, \\ & && \mathbf{H} \in \Omega_h := \mathbb{R}_+^{r \times n}. \end{aligned} \quad (10)$$

Based on the SSNMF framework (10), we introduce the following four SSNMF models as follows:

- **Row-sparse NMF** with  $\ell_{2,0}$ -norm constraint (NMF- $\ell_{20}$ ). When  $\rho = 0$ , the penalty term has no effect and Eq. (10) reduces to NMF- $\ell_{20}$ .
- **Row-sparse ONMF** with  $\ell_{2,0}$ -norm constraint (ONMF- $\ell_{20}$ ). When  $\rho$  is large enough, Eq. (10) reduces to ONMF- $\ell_{20}$ . As  $\rho \rightarrow \infty$  in Eq. (10), the impact of the penalty grows, and the estimated  $\mathbf{H}$  will approach a nonnegative orthogonal matrix.
- **Column-sparse NMF** with  $\ell_{c,0}$ -norm constraint (NMF- $\ell_{c0}$ ). When  $\rho = 0$  and  $\Omega_w$  is defined in Eq. (8), Eq. (10) reduces to NMF- $\ell_{c0}$ .
- **Column-sparse ONMF** with  $\ell_{c,0}$ -norm constraint (ONMF- $\ell_{c0}$ ). When  $\rho$  is large enough and  $\Omega_w$  is defined in Eq. (8), Eq. (10) reduces to ONMF- $\ell_{c0}$ .

We first present Proposition 1 to clarify the relationship between the solutions of Eq. (10) and Eq. (7), whose proof is shown in the appendix A-B. Proposition 1 implies that we can solve Eq. (7) by repeatedly solving Eq. (10) with a gradually increasing  $\rho$ . Therefore, the key to solve the above four models (NMF- $\ell_{20}$ , NMF- $\ell_{c0}$ , ONMF- $\ell_{20}$ , and ONMF- $\ell_{c0}$ ) is to solve the SSNMF framework (10).

**Proposition 1.** *Let  $(\mathbf{W}^*, \mathbf{H}^*)$  be a local minimizer of Eq. (10). Then for any  $\rho > 0$ ,  $(\mathbf{W}^*, \mathbf{H}^*)$  is also the feasible and local minimizer of Eq. (7).*

Alternating minimization is a popular strategy to solve the constrained and penalized matrix factorization problem in Eq. (10). Recently, a PALM algorithm has been proposed to solve a class of constrained and penalized matrix factorization problems which satisfies KL property [22]. We present Theorem 1 to show that Eq. (10) satisfies KL property, such that the PALM algorithm can be used to solve it.

**Theorem 1.**  $\Phi = F(\mathbf{W}, \mathbf{H}) + \delta_{\mathbf{W} \geq 0} + \delta_{\mathbf{H} \geq 0} + \delta_{\|\mathbf{W}\|_{2,0} \leq k}$  is a semi-algebraic function and it satisfies the KL property, where  $F = \frac{1}{2} \|\mathbf{X} - \mathbf{W}\mathbf{H}\|_F^2 + \frac{\rho}{2} \sum_{j=1}^n \left( (1^T \mathbf{h}_j)^2 - \|\mathbf{h}_j\|_2^2 \right)$ , and  $\delta_{\|\mathbf{W}\|_{2,0} \leq k}$  is zero if  $\|\mathbf{W}\|_{2,0} \leq k$ , otherwise  $+\infty$ .

*Proof.* Remark 8 in [22] shows the following conclusions: (1)  $\|\cdot\|_0$  and  $\|\cdot\|_2$  are semi-algebraic functions; (2) The indicator function in a semi-algebraic set is semi-algebraic; (3) Any composition of semi-algebraic function remains to be semi-algebraic; (4) The finite sums of semi-algebraic functions remain semi-algebraic. Based the above conclusions, we know that (1)  $F$ ,  $\delta_{\mathbf{W} \geq 0}$  and  $\delta_{\mathbf{H} \geq 0}$  are semi-algebraic functions, respectively; (2)  $\delta_{\|\mathbf{W}\|_{2,0} \leq k}$  is a semi-algebraic function because  $\|\mathbf{W}\|_{2,0} := \|(\|\mathbf{w}^1\|_2, \dots, \|\mathbf{w}^p\|_2)\|_0$  is a composition of semi-algebraic function  $\|\cdot\|_0$  and  $\|\cdot\|_2$ . Thus, we prove that  $\Phi$  is a semi-algebraic function because it is a sum of four semi-algebraic functions. In addition, we observe that  $\Phi$  is a proper and lower semicontinuous function. Based on the Theorem 3 in [22], a proper, lower semicontinuous and semi-algebraic function  $\Phi$  satisfies the KL property. The relevant mathematical definitions are shown in Appendix A-A.  $\square$

By the way, the proof of Theorem 1 also implies that the  $\ell_{2,0}$ -norm satisfies the KL property such that the PALM can be used to solve a class of optimization problems with  $\ell_{2,0}$ -norm constraint.

## IV. OPTIMIZATION METHOD

### A. PALM and maPALM

We first introduce a general constrained and penalized matrix factorization model as follows:

$$\begin{aligned} & \underset{\mathbf{W}, \mathbf{H}}{\text{minimize}} && F(\mathbf{W}, \mathbf{H}) = \frac{1}{2} \|\mathbf{X} - \mathbf{W}\mathbf{H}\|_F^2 + \phi(\mathbf{W}) + \varphi(\mathbf{H}) \\ & \text{subject to} && \mathbf{W} \in \Omega_w, \mathbf{H} \in \Omega_h. \end{aligned} \quad (11)$$

Obviously, the SSNMF framework in Eq. (10) is a special case of Eq. (11). To solve Eq. (11) using the PALM algorithm, we need to perform a projected gradient descent step with respect to  $\mathbf{H}$  and  $\mathbf{W}$  for  $t = 1, 2, \dots$ :

$$\begin{aligned} \mathbf{H}^{t+1} &= \mathcal{P}_{\mathbf{H} \in \Omega_H} \left\{ \mathbf{H}^t - \frac{1}{d_H^t} \nabla_{\mathbf{H}} F(\mathbf{W}^t, \mathbf{H}^t) \right\}, \\ \mathbf{W}^{t+1} &= \mathcal{P}_{\mathbf{W} \in \Omega_W} \left\{ \mathbf{W}^t - \frac{1}{d_W^t} \nabla_{\mathbf{W}} F(\mathbf{W}^t, \mathbf{H}^{t+1}) \right\}, \end{aligned}$$

where  $d_H^t$  and  $d_W^t$  are two step-size parameters,  $\mathcal{P}_{\mathbf{H} \in \Omega_H} \{\cdot\}$  and  $\mathcal{P}_{\mathbf{W} \in \Omega_W} \{\cdot\}$  are two projection operations onto  $\Omega_H$  and  $\Omega_W$ , respectively. A basic algorithmic framework for solving Eq. (11) is shown in Algorithm 1.

Because of the linearization of PALM, its convergence speed may be slow. Accelerated proximal gradient method has been

widely used to solve convex optimization problems. Unfortunately, if the non-monotone accelerated proximal gradient uses a bad extrapolation for some non-convex problems, then it may not converge to a critical point [27]. Fortunately, the monotone accelerated method guarantees convergence for a non-convex problem by ensuring that its objective function value decreases every iteration [27, 28].

---

**Algorithm 1** PALM for solving Eq. (11).

---

**Require:**  $\mathbf{X} \in \mathbb{R}^{p \times n}$  and  $\epsilon > 0$ .

**Ensure:**  $\mathbf{W} \in \mathbb{R}^{p \times r}$  and  $\mathbf{H} \in \mathbb{R}^{r \times n}$ .

- 1: Initialize  $(\mathbf{W}^0, \mathbf{H}^0)$  and set  $t = 0$
  - 2: **repeat**
  - 3:   Compute  $d_H^t$
  - 4:    $\mathbf{H}^{t+1} = \mathcal{P}_{H \in \Omega_H} \left\{ \mathbf{H}^t - \frac{1}{d_H^t} \nabla_H F(\mathbf{W}^t, \mathbf{H}^t) \right\}$
  - 5:   Compute  $d_W^t$
  - 6:    $\mathbf{W}^{t+1} = \mathcal{P}_{W \in \Omega_W} \left\{ \mathbf{W}^t - \frac{1}{d_W^t} \nabla_W F(\mathbf{W}^t, \mathbf{H}^{t+1}) \right\}$
  - 7:    $t = t + 1$
  - 8: **until**  $\frac{\|(\mathbf{W}^t, \mathbf{H}^t) - (\mathbf{W}^{t-1}, \mathbf{H}^{t-1})\|}{\|(\mathbf{W}^{t-1}, \mathbf{H}^{t-1})\|} < \epsilon$
  - 9: **return**  $\mathbf{W} := \mathbf{W}^t$  and  $\mathbf{H} := \mathbf{H}^t$ .
- 

---

**Algorithm 2** maPALM for solving Eq. (11).

---

**Require:**  $\mathbf{X} \in \mathbb{R}^{p \times n}$ ,  $\epsilon > 0$  and  $\omega_0$ .

**Ensure:**  $\mathbf{W} \in \mathbb{R}^{p \times r}$  and  $\mathbf{H} \in \mathbb{R}^{r \times n}$ .

- 1: Initialize  $(\mathbf{W}^{-1}, \mathbf{H}^{-1}) = (\mathbf{W}^0, \mathbf{H}^0)$  and  $t = 0$
  - 2: **repeat**
  - 3:    $\widetilde{\mathbf{H}}^t = \mathbf{H}^t + \omega_t(\mathbf{H}^t - \mathbf{H}^{t-1})$
  - 4:   Compute  $d_H^t$
  - 5:    $\widetilde{\mathbf{H}}^{t+1} = \mathcal{P}_{H \in \Omega_H} \left\{ \widetilde{\mathbf{H}}^t - \frac{1}{d_H^t} \nabla_H F(\mathbf{W}^t, \widetilde{\mathbf{H}}^t) \right\}$
  - 6:    $\widetilde{\mathbf{W}}^t = \mathbf{W}^t + \omega_t(\mathbf{W}^t - \mathbf{W}^{t-1})$
  - 7:   Compute  $d_W^t$
  - 8:    $\widetilde{\mathbf{W}}^{t+1} = \mathcal{P}_{W \in \Omega_W} \left\{ \widetilde{\mathbf{W}}^t - \frac{1}{d_W^t} \nabla_W F(\widetilde{\mathbf{W}}^t, \widetilde{\mathbf{H}}^{t+1}) \right\}$
  - 9:   **if**  $F(\widetilde{\mathbf{W}}^{t+1}, \widetilde{\mathbf{H}}^{t+1}) \leq F(\mathbf{W}^t, \mathbf{H}^t)$  **then**
  - 10:      $(\mathbf{W}^{t+1}, \mathbf{H}^{t+1}) := (\widetilde{\mathbf{W}}^{t+1}, \widetilde{\mathbf{H}}^{t+1})$
  - 11:   **else**
  - 12:     update  $(\mathbf{W}^{t+1}, \mathbf{H}^{t+1})$  using Eq. (12)
  - 13:   **end if**
  - 14:   Compute  $\omega_t$  and set  $t = t + 1$
  - 15: **until**  $\frac{\|(\mathbf{W}^t, \mathbf{H}^t) - (\mathbf{W}^{t-1}, \mathbf{H}^{t-1})\|}{\|(\mathbf{W}^{t-1}, \mathbf{H}^{t-1})\|} < \epsilon$
  - 16: **return**  $\mathbf{W} := \mathbf{W}^t$  and  $\mathbf{H} := \mathbf{H}^t$ .
- 

To this end, we develop a monotone accelerated PALM framework and its details is shown in Algorithm 2, which can be regarded as a special case of the block prox-linear method [29]. Similarly, maPALM ensures the objective function value decreases. Reference [27, 29],  $\omega_k$  ( $k = 0, 1, 2, \dots$ ) in Algorithm 2 is dynamically updated by

$$\omega_k = \frac{\tau_k - 1}{\tau_{k+1}}, \quad (13)$$

where  $\tau_0 = 1$  and  $\tau_{k+1} = \left(1 + \sqrt{1 + 4\tau_k^2}\right)/2$ .

We note that maPALM reduces to PALM when  $\omega_t = 0$  for all  $t$ . Especially, NMF- $\ell_{20}$  and NMF- $\ell_{c0}$  can be solved by Algorithm 1 and 2 with  $\phi(\mathbf{W}) = \varphi(\mathbf{H}) = 0$ . In addition,

the conclusion of Proposition 1 implies that we can solve Eq. (7) by repeatedly solving Eq. (10) with a gradually increasing  $\rho$ . To this end, we can develop an efficient algorithm for ONMF- $\ell_{20}$  or ONMF- $\ell_{c0}$  by turning ONMF- $\ell_{20}$  or ONMF- $\ell_{c0}$  into a sequence subproblems.

In summary, the key to solving NMF- $\ell_{20}$ , NMF- $\ell_{c0}$ , ONMF- $\ell_{20}$  and ONMF- $\ell_{c0}$  is to solve the SSNMF framework in Eq. (10). Below we show the details of using the maPALM algorithm to solve it.

### B. Solve SSNMF with $\ell_{2,0}$ -norm constraint

We use maPALM to solve a row-sparse SSNMF in Eq. (10) with  $\ell_{2,0}$ -norm constraint:

$$\begin{aligned} \underset{\mathbf{W}, \mathbf{H}}{\text{minimize}} \quad & \frac{1}{2} \|\mathbf{X} - \mathbf{W}\mathbf{H}\|_F^2 + \frac{\rho}{2} \sum_{j=1}^n \left( (\mathbf{1}^T \mathbf{h}_j)^2 - \|\mathbf{h}_j\|_2^2 \right) \\ \text{subject to} \quad & \mathbf{W} \in \mathbb{R}_+^{p \times r}, \|\mathbf{W}\|_{2,0} \leq k, \mathbf{H} \in \mathbb{R}_+^{r \times n}. \end{aligned} \quad (14)$$

Let  $F = \frac{1}{2} \|\mathbf{X} - \mathbf{W}\mathbf{H}\|_F^2 + \frac{\rho}{2} \sum_{j=1}^n \left( (\mathbf{1}^T \mathbf{h}_j)^2 - \|\mathbf{h}_j\|_2^2 \right)$ , then

$$\nabla_H F = \mathbf{W}^T \mathbf{W} \mathbf{H} - \mathbf{W}^T \mathbf{X} + \rho \mathbf{1}_{r \times r} \mathbf{H} - \rho \mathbf{H}, \quad (15a)$$

$$\nabla_W F = \mathbf{W} \mathbf{H} \mathbf{H}^T - \mathbf{X} \mathbf{H}^T. \quad (15b)$$

And the Hessian matrices of  $F$  with respect to  $\mathbf{W}$  and  $\mathbf{H}$  are

$$\nabla_W^2 F = (\mathbf{H} \mathbf{H}^T) \otimes \mathbf{I}_p, \quad (16a)$$

$$\nabla_H^2 F = \mathbf{I}_p \otimes (\mathbf{W}^T \mathbf{W} + \rho \mathbf{1}_{r \times r} - \rho \mathbf{I}_r). \quad (16b)$$

where  $\otimes$  is Kronecker product and  $\mathbf{I}_p \in \mathbb{R}^{p \times p}$  is an identity matrix. To use maPALM to solve Eq. (14), we need to calculate Lipschitz constant to determine the step size. The Lemma 2 in reference [30] shows that  $\nabla_W F$  and  $\nabla_H F$  are Lipschitz continuous, the Lipschitz constant of  $\nabla_W F$  is the largest singular value of  $\nabla_W^2 F$ , i.e.,  $L_W = \|\mathbf{H} \mathbf{H}^T\|_2$ , and the Lipschitz constant of  $\nabla_H F$  is the largest singular value of  $\nabla_H^2 F$ , i.e.,  $L_H = \|\mathbf{W}^T \mathbf{W} + \rho \mathbf{1}_{r \times r} - \rho \mathbf{I}_r\|_2$ . Thus, we can set  $d_W^t = L_W$  and  $d_H^t = L_H$  in Algorithms 1 to 2.

**1) Optimize  $\mathbf{W}$ .** Specifically, to obtain the update of  $\mathbf{W}$  for Eq. (14), we need to solve a proximal map  $\mathbf{W}^{t+1} := \mathcal{P}_{W \in \Omega_W} \{\overline{\mathbf{W}}\}$  as follows:

$$\begin{aligned} \underset{\mathbf{W}}{\text{minimize}} \quad & \|\mathbf{W} - \overline{\mathbf{W}}\|_F^2 \\ \text{subject to} \quad & \mathbf{W} \in \mathbb{R}_+^{p \times r}, \|\mathbf{W}\|_{2,0} \leq k, \end{aligned} \quad (17)$$

where  $\overline{\mathbf{W}} := \mathbf{W}^t - \frac{1}{d_W^t} \nabla_W F(\mathbf{W}^t, \mathbf{H}^t)$ . We propose Proposition 2 to solve the proximal map. To this end, we introduce the following mathematical definitions.

**Definition 1.** SupportNorm( $\mathbf{W}, k$ ) is a set of indices of  $\mathbf{z}$  with the largest  $k$  values where  $\mathbf{z} = (\|\mathbf{w}^1\|, \dots, \|\mathbf{w}^p\|)$  and  $\mathbf{w}^i$  denotes  $i$ -th row of  $\mathbf{W}$ .

**Definition 2.** For a given matrix  $\mathbf{W} \in \mathbb{R}^{p \times r}$ ,  $\text{RS}_k(\mathbf{W})$  is also a  $p \times r$  matrix which is defined as:

$$[\text{RS}_k(\mathbf{W})]_{ij} = \begin{cases} W_{ij}, & \text{if } i \in \text{SupportNorm}(\mathbf{W}, k), \\ 0, & \text{otherwise,} \end{cases} \quad (18)$$

where  $\text{SupportNorm}(\mathbf{W}, k)$  is defined in Definition 1.  $\text{RS}_k(\mathbf{W})$  only keeps  $k$  non-zero rows with the largest  $\ell_2$ -norm values in  $\mathbf{W}$ .

**Definition 3.** For a given matrix  $\mathbf{W} \in \mathbb{R}^{p \times r}$ ,  $P_+(\mathbf{W})$  is defined as follows:

$$[P_+(\mathbf{W})]_{ij} = \begin{cases} W_{ij}, & \text{if } W_{ij} > 0 \forall i \text{ and } j, \\ 0, & \text{otherwise.} \end{cases} \quad (19)$$

**Proposition 2.** (Proximal map formula of  $\mathbf{W}$  for ONMF- $\ell_{20}$ ) Let  $\overline{\mathbf{W}} \in \mathbb{R}^{p \times r}$ , then Eq. (17) has a closed-form solution

$$\mathcal{P}_{W \in \Omega_W} \{\overline{\mathbf{W}}\} := \text{RS}_k(P_+(\overline{\mathbf{W}})), \quad (20)$$

where  $\text{RS}_k(\cdot)$  and  $P_+(\cdot)$  are defined in Definition 2 and 3, respectively.

*Proof.* Suppose that the optimal solution of Eq. (17) is  $\widehat{\mathbf{W}}$ , then we can easily observe that  $\widehat{W}_{ij}$  must be zero when  $\overline{W}_{ij} < 0$ . So, Eq. (17) is equivalent to

$$\underset{\mathbf{W}}{\text{minimize}} \|\mathbf{W} - P_+(\overline{\mathbf{W}})\|_F^2, \text{ subject to } \|\mathbf{W}\|_{2,0} \leq k.$$

Due to the constraint  $\|\mathbf{W}\|_{2,0} \leq k$ , the optimal solution only keeps up to  $k$  non-zero rows. So, Eq. (17) has a closed-form solution  $\text{RS}_k(P_+(\overline{\mathbf{W}}))$ .  $\square$

**2) Optimize  $\mathbf{H}$ .** To obtain the update of  $\mathbf{H}$  for Eq. (14), we need to solve a proximal map  $\mathbf{H}^{t+1} := \mathcal{P}_{H \in \Omega_H} \{\overline{\mathbf{H}}\}$  as follows:

$$\underset{\mathbf{H}}{\text{minimize}} \|\mathbf{H} - \overline{\mathbf{H}}\|_F^2, \text{ subject to } \mathbf{H} \in \mathbb{R}_+^{r \times n}, \quad (21)$$

where  $\overline{\mathbf{H}} := \mathbf{H}^t - \frac{1}{d_H^t} \nabla_H F(\mathbf{W}^{t+1}, \mathbf{H}^t)$ . We propose the following Proposition 3 to solve the above problem.

**Proposition 3.** (Proximal map formula of  $\mathbf{H}$  for ONMF- $\ell_{20}$ ) Let  $\overline{\mathbf{H}} \in \mathbb{R}^{r \times n}$ , then (21) has a closed-form solution:

$$\mathcal{P}_{H \in \Omega_H} \{\overline{\mathbf{H}}\} := P_+(\overline{\mathbf{H}}), \quad (22)$$

where  $P_+(\cdot)$  is defined in Definition 3.

**3) Algorithm for solving Eq. (14).** Based on the Propositions 2 and 3, we develop a maPALM algorithm to solve Eq. (14) and the detailed algorithm is given in Algorithm 3. To maintain monotonicity, maPALM needs to use a suitable  $\omega_t$  by checking the objective function value. If the objective function value becomes larger, then we obtain the update rule based on the traditional projected gradient descent method. Monotonicity can ensure that Algorithm 3 converges to a critical point for any initial point. The following Theorem 2 gives the details on the convergence analysis of Algorithm 3.

**Algorithm for NMF- $\ell_{20}$ .** Algorithm 3 with  $\rho = 0$  can effectively solve NMF- $\ell_{20}$ .

**Initialization.** We can adopt two ways to generate the initial point of Algorithm 3. One is to use the random vectors from a standard normal distribution to initialize  $\mathbf{W}$  and  $\mathbf{H}$ . The other is to use the solution  $\mathbf{W}$  and  $\mathbf{H}$  derived by the traditional NMF to initialize them. The second way is a good guess. So, if not specified, we use the second way to initialize by default.

**Algorithm 3** maPALM for solving Eq. (14).

**Require:**  $\mathbf{X} \in \mathbb{R}^{p \times n}$ ,  $\rho \geq 0$ ,  $\epsilon > 0$ ,  $k$  (nonzero rows).

**Ensure:**  $\mathbf{W} \in \mathbb{R}^{p \times r}$  and  $\mathbf{H} \in \mathbb{R}^{r \times n}$ .

- 1: Initialize  $(\mathbf{W}^{-1}, \mathbf{H}^{-1}) = (\mathbf{W}^0, \mathbf{H}^0)$ ,  $\tau_0 = 1$  and  $t = 0$
- 2: **repeat**
- 3:   Compute  $\omega_t = \frac{\tau_t - 1}{\tau_{t+1}}$  where  $\tau_{t+1} = \frac{1 + \sqrt{1 + 4\tau_t^2}}{2}$
- 4:    $\widetilde{\mathbf{H}}^t = \mathbf{H}^t + \omega_t(\mathbf{H}^t - \mathbf{H}^{t-1})$
- 5:    $d_H^t = \|(\mathbf{W}^t)^T(\mathbf{W}^t) + \rho \mathbf{1}_{r \times r} - \rho \mathbf{I}_r\|_2$
- 6:    $\mathbf{H}^{t+1} = P_+(\widetilde{\mathbf{H}}^t - \frac{1}{d_H^t} \nabla_H F(\mathbf{W}^t, \widetilde{\mathbf{H}}^t))$
- 7:    $\widetilde{\mathbf{W}}^t = \mathbf{W}^t + \omega_t(\mathbf{W}^t - \mathbf{W}^{t-1})$
- 8:    $d_W^t = \|(\mathbf{H}^{t+1})(\mathbf{H}^{t+1})^T\|_2$
- 9:    $\mathbf{W}^{t+1} = \text{RS}_k(\widetilde{\mathbf{W}}^t - \frac{1}{d_W^t} \nabla_W F(\widetilde{\mathbf{W}}^t, \mathbf{H}^{t+1}))$
- 10:   **if**  $F(\widetilde{\mathbf{W}}^{t+1}, \widetilde{\mathbf{H}}^{t+1}) \leq F(\mathbf{W}^t, \mathbf{H}^t)$  **then**
- 11:      $(\mathbf{W}^{t+1}, \mathbf{H}^{t+1}) := (\widetilde{\mathbf{W}}^{t+1}, \widetilde{\mathbf{H}}^{t+1})$
- 12:   **else**
- 13:      $d_H^t = \|(\mathbf{W}^t)^T(\mathbf{W}^t) + \rho \mathbf{1}_{r \times r} - \rho \mathbf{I}_r\|_2$
- 14:      $\mathbf{H}^{t+1} = P_+(\mathbf{H}^t - \frac{1}{d_H^t} \nabla_H F(\mathbf{W}^t, \mathbf{H}^t))$
- 15:      $d_W^t = \|(\mathbf{H}^{t+1})(\mathbf{H}^{t+1})^T\|_2$
- 16:      $\mathbf{W}^{t+1} = \text{RS}_k(\mathbf{W}^t - \frac{1}{d_W^t} \nabla_W F(\mathbf{W}^t, \mathbf{H}^{t+1}))$
- 17:   **end if**
- 18:    $t = t + 1$
- 19: **until**  $\frac{\|(\mathbf{W}^t, \mathbf{H}^t) - (\mathbf{W}^{t-1}, \mathbf{H}^{t-1})\|}{\|(\mathbf{W}^{t-1}, \mathbf{H}^{t-1})\|} < \epsilon$
- 20: **return**  $\mathbf{W} := \mathbf{W}^t$  and  $\mathbf{H} := \mathbf{H}^t$ .

**Step-size.** We can use a fixed value of the step-size  $1/d_H^t$  and  $1/d_W^t$  in Algorithm 3, and also try to perform an approximate backtracking line search from  $t \in (0, 0.5)$ . Specifically, we use the fixed  $d_W^t = L_W$  and  $d_H^t = L_H$  in this paper.

**4) Computation cost.** The computational complexity of Algorithm 3 depends on the number of iterations. At each iteration, only two simple closed-form solutions need to be computed with respect to  $\mathbf{H}$  and  $\mathbf{W}$  in the steps 6 and 9, respectively. For each update of  $\mathbf{H}$ , the most costly step is the calculation of  $\nabla_H F$ , which requires a computation cost of  $O(pr^2 + nr^2)$ . For each update of  $\mathbf{W}$ , the most costly steps is the calculation of  $\nabla_W F$ , which requires a computation cost of  $O(pr^2 + nr^2 + pnr)$ . In addition, the calculation of objective function value requires a computation cost of  $O(pnr + pn + rn)$ . Thus, each iteration of Algorithm 3 requires a computation cost of  $O(pr^2 + nr^2 + pnr)$ .

**5) Convergence analysis.** Based on some results from references [22, 29], we propose the following Theorem 2 to show that Algorithm 3 globally converges to a critical point.

**Theorem 2.** (Global convergence of Algorithm 3) Let  $\{(\mathbf{W}^{(i)}, \mathbf{H}^{(i)})\}_{i=1}^\infty$  be a sequence generated from any starting point  $(\mathbf{W}^{(0)}, \mathbf{H}^{(0)})$  by Algorithm 3. If  $\{(\mathbf{W}^{(i)}, \mathbf{H}^{(i)})\}$  are bounded, then the objective is non-increasing and the sequence has finite length and converges to a critical point.

*Proof.* Based on Theorem 1, the objective function  $\Phi$  is a semi-algebraic function and satisfies the KL property. Checking the assumptions of Theorem 2 in reference [29], we observe that all assumptions required in Algorithm 3 are clearly satisfied. So, we have Theorem 2.  $\square$

### C. Solve SSNMF with $\ell_{c,0}$ -norm constraint

Let  $\Omega_w := \{\mathbf{W} \in \mathbb{R}_+^{p \times r} : \|\mathbf{w}_j\|_0 \leq k, \forall j\}$  in Eq. (10), we consider a column-wise SSNMF with  $\ell_{c,0}$ -norm constraint by using  $\ell_0$ -norm for each column of  $\mathbf{W}$  as follows:

$$\begin{aligned} & \underset{\mathbf{W}, \mathbf{H}}{\text{minimize}} && \frac{1}{2} \|\mathbf{X} - \mathbf{W}\mathbf{H}\|_F^2 + \frac{\rho}{2} \sum_{j=1}^n \left( (\mathbf{1}^T \mathbf{h}_j)^2 - \|\mathbf{h}_j\|_2^2 \right) \\ & \text{subject to} && \mathbf{W} \in \mathbb{R}_+^{p \times r}, \|\mathbf{w}_j\|_0 \leq k, \forall j, \mathbf{H} \in \mathbb{R}_+^{r \times n}. \end{aligned} \quad (23)$$

To obtain the update of  $\mathbf{W}$ , we need to solve a proximal map  $\mathbf{W}^{t+1} := \mathcal{P}_{\mathbf{W} \in \Omega_w} \{\overline{\mathbf{W}}\}$ :

$$\begin{aligned} & \underset{\mathbf{W}}{\text{minimize}} && \|\mathbf{W} - \overline{\mathbf{W}}\|_F^2 \\ & \text{subject to} && \mathbf{W} \in \mathbb{R}_+^{p \times r}, \|\mathbf{w}_j\|_0 \leq k, \forall j. \end{aligned} \quad (24)$$

**Definition 4.** For a given matrix  $\mathbf{W} \in \mathbb{R}^{p \times r}$ ,  $\text{CS}_k(\mathbf{W}) \in \mathbb{R}^{p \times r}$  ( $k \leq p$ ) is defined as:

$$[\text{CS}_k(\mathbf{W})]_{ij} = \begin{cases} W_{ij}, & j \in \text{SupportNorm}(\mathbf{w}_j, k), \\ 0, & \text{otherwise,} \end{cases} \quad (25)$$

where  $\mathbf{w}_j$  denotes  $j$ -th column of  $\mathbf{W}$  and  $\text{SupportNorm}(\cdot, k)$  is defined in Definition 1.

**Proposition 4.** (Proximal map formula of  $\mathbf{W}$  for ONMF- $\ell_{c0}$ ) Let  $\overline{\mathbf{W}} \in \mathbb{R}^{p \times r}$ , then Eq. (24) has a closed-form solution:

$$\mathcal{P}_{\mathbf{W} \in \Omega_w} \{\overline{\mathbf{W}}\} := \text{CS}_k(P_+(\overline{\mathbf{W}})), \quad (26)$$

where  $\text{CS}_k(\cdot)$  and  $P_+(\cdot)$  are defined in Definition 4 and 3, respectively.

*Proof.* Suppose that the optimal solution of Eq. (24) is  $\widehat{\mathbf{W}}$ , then we can observe that  $\widehat{W}_{ij}$  must be zero when  $\overline{W}_{ij} < 0$ . So, Eq. (24) is equivalent to

$$\underset{\mathbf{W}}{\text{minimize}} \|\mathbf{W} - P_+(\overline{\mathbf{W}})\|_F^2 \text{ subject to } \|\mathbf{w}_j\|_0 \leq k, \forall j.$$

Due to the constraint  $\|\mathbf{w}_j\|_0 \leq k$ , the optimal solution only keeps  $k$  non-zero elements with the largest absolute values for each column of  $\mathbf{W}$ . So, Eq. (24) has a closed-form solution  $\text{CS}_k(P_+(\overline{\mathbf{W}}))$ .  $\square$

**Algorithm for solving Eq. (23).** Based on Proposition 4, we can solve Eq. (23) by replacing  $\text{CS}_k(\cdot)$  with  $\text{RS}_k(\cdot)$  in Algorithm 3. Similar to Theorem 2, the variant of Algorithm 3 has theoretical convergence guarantees.

### D. Solve ONMF- $\ell_{20}$ and ONMF- $\ell_{c0}$

We develop an efficient algorithm for ONMF- $\ell_{20}$  by turning it into a series of constrained and penalized matrix factorization problems, i.e., Eq. (14) with different  $\rho$ , which can be solved by the PALM or maPALM algorithm. The detailed algorithm is given in Algorithm 4.

In Algorithm 4, we set the default parameters  $\rho = 0.1$ ,  $\gamma = 1.5$ , and  $K = 10$ . As  $\rho \rightarrow \infty$  in the step 4 of Algorithm 4, the impact of the penalty grows, and the estimated  $\mathbf{H}$  will approach a non-negative orthogonal matrix. Finally, we can also use a method similar to Algorithm 4 to solve ONMF- $\ell_{c0}$  by turning it into a series of constrained and penalized matrix factorization problems, i.e., Eq. (23) with different  $\rho$ .

---

### Algorithm 4 ONMF- $\ell_{20}$ Algorithm

---

**Require:**  $\mathbf{X} \in \mathbb{R}^{p \times n}$ ,  $\rho \geq 0$  and  $\gamma > 1$ .

**Ensure:**  $\mathbf{W} \in \mathbb{R}^{p \times r}$  and  $\mathbf{H} \in \mathbb{R}^{r \times n}$ .

- 1: Initialize  $(\mathbf{W}^0, \mathbf{H}^0)$
  - 2: **for**  $k = 1, 2, \dots, K$  **do**
  - 3:   Obtain  $(\mathbf{W}, \mathbf{H})$  by solving Eq. (15) with  $\rho$  using PALM or maPALM with the initialization  $(\mathbf{W}^0, \mathbf{H}^0)$ .
  - 4:    $\rho := \gamma\rho$  and  $(\mathbf{W}^0, \mathbf{H}^0) := (\mathbf{W}, \mathbf{H})$
  - 5: **end for**
  - 6: **return**  $\mathbf{W}$  and  $\mathbf{H}$ .
- 

## V. EXPERIMENTS

We evaluate the effectiveness of these proposed SSNMF methods for clustering task and compare them with state-of-the-art matrix factorization, k-means and two sparse k-means methods on the synthetic and scRNA-seq data. All competing methods are listed as follows:

- ONMF- $\ell_{20}$ : ONMF with  $\ell_{2,0}$ -norm constraint (Eq. 7).
- ONMF- $\ell_{20-\rho}$ : ONMF- $\ell_{20}$  with a fixed  $\rho$  (Eq. 14).
- ONMF- $\ell_{c0}$ : column-wise sparse ONMF (Eq. 23).
- ONMF- $\ell_0$ : ONMF with  $\ell_0$ -norm constraint.
- NMF- $\ell_{20}$ : NMF with  $\ell_{2,0}$ -norm constraint.
- ONMF: Orthogonal NMF [25].
- NMF: Non-negative Matrix factorization [31].
- NMF- $\ell_0$ : NMF with  $\ell_0$ -norm constraint [22].
- NMF- $\ell_{c0}$ : Column-wise sparse NMF [32].
- Kmeans: A baseline unsupervised method.
- Kmeans- $\ell_1$ : Sparse  $k$  means with  $\ell_1$  penalty in [33].
- Kmeans- $\ell_0$ : Sparse  $k$  means with  $\ell_\infty/\ell_0$  penalty in [34].

Wherein the proposed SSNMF methods in this study include ONMF- $\ell_{20}$ , ONMF- $\ell_{20-\rho}$ , ONMF- $\ell_{c0}$ , ONMF- $\ell_0$  and NMF- $\ell_{20}$ .

### A. Evaluation metrics

To evaluate the clustering performance, we use three metrics including NMI (Normalized Mutual Information) [35], Purity and Entropy [14]. Suppose  $c$  is the number of clustering clusters and  $d$  is the number of true categories. Then NMI is defined as

$$\text{NMI} = \frac{\sum_{l=1}^c \sum_{h=1}^d t_{l,h} \log\left(\frac{n \cdot t_{l,h}}{t_l \hat{t}_h}\right)}{\sqrt{(\sum_{l=1}^c t_l \log \frac{t_l}{n}) (\sum_{h=1}^d \hat{t}_h \log \frac{\hat{t}_h}{n})}}, \quad (27)$$

Purity is defined as

$$\text{Purity} = \frac{1}{n} \sum_{l=1}^c \max_{1 \leq h \leq d} t_{l,h}, \quad (28)$$

Entropy is defined as

$$\text{Entropy} = \frac{1}{n \log_2 d} \sum_{l=1}^c \sum_{h=1}^d t_{l,h} \log_2 \frac{t_{l,h}}{t_l}, \quad (29)$$

where  $n$  is the number of considered samples,  $t_l$  is the number of samples from the  $l$ -th cluster  $C_l$ , which is obtained by clustering method and  $\hat{t}_h$  is the number of samples from the  $h$ -th ground truth class  $G_h$ .  $t_{l,h}$  denotes the number of

overlapping samples between  $C_l$  and  $G_h$ . The larger the values of NMI and purity or the smaller the value of entropy, the better the clustering performance.

### B. Application to synthetic data

We generate a synthetic data  $\mathbf{X} \in \mathbb{R}^{p \times n}$  where  $p = 500$  features and  $n = 60$  samples from three true classes. Firstly, the elements in  $\mathbf{X}$  satisfy  $X_{ij} \sim N(0, 1)$  ( $1 \leq i \leq 60, 1 \leq j \leq 20$ ),  $X_{ij} \sim N(0, 1)$  ( $31 \leq i \leq 90, 21 \leq j \leq 40$ ) and  $X_{ij} \sim N(0, 1)$  ( $61 \leq i \leq 120, 41 \leq j \leq 60$ ) and  $X_{ij} \sim 0.9 * N(0, 1)$  for the other  $i$  and  $j$ , where  $N(0, 1)$  denotes standard normal distribution. Secondly, we set  $X_{ij} := |X_{ij}|$  for any  $i$  and  $j$  to ensure every element in the final synthetic data matrix  $\mathbf{X}$  is positive (see Figure 2A).

First of all, we show the convergence performance of PALM and maPALM when they are used to solve ONMF- $\ell_{20}$  model in Eq. (14) on the synthetic data (Figure 2B). We find that the convergence speed of maPALM is significantly faster than that of PALM.

Secondly, to validate the effectiveness of our proposed methods to perform feature selection, we compare them with state-of-the-art methods on the synthetic data. The parameters of these compared methods are carefully adjusted to give their best performances and all methods are repeated 10 times using different initial points for comparison. The corresponding NMI scores are recorded for each method and the methods with higher NMI averages are regarded as more accurate ones. We find that the SSNMF methods including ONMF- $\ell_{20}$  and NMF- $\ell_{20}$  outperform other algorithms in terms of NMI (Figure 3). Interestingly, we also find that as  $\rho$  becomes larger in the Algorithm 3, the orthogonality level of estimated  $\mathbf{H}$  is better, such that the clustering performance is better (Figure 4). This result implies that it is possible to improve the clustering accuracy by adding the non-negative and orthogonal constraint in SSNMF model.

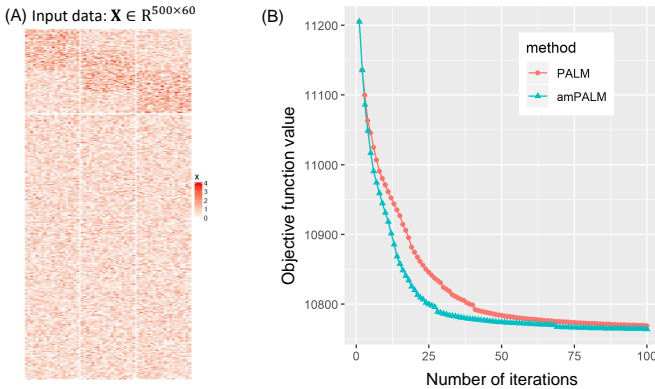


Figure 2. Results on the synthetic data. (A) Heatmap showing the synthetic data. (B) Convergence performance of PALM and maPALM for ONMF- $\ell_{20}$  with a fixed  $\rho = 0.5$ .

Finally, we evaluate whether ONMF can detect outliers by sorting the values of estimated  $\mathbf{H}$ . To this end, we generate a new synthetic data  $\mathbf{X} \in \mathbb{R}^{p \times n}$  where  $p = 500$  features and  $n = 60$  samples from three classes. Firstly, the elements in

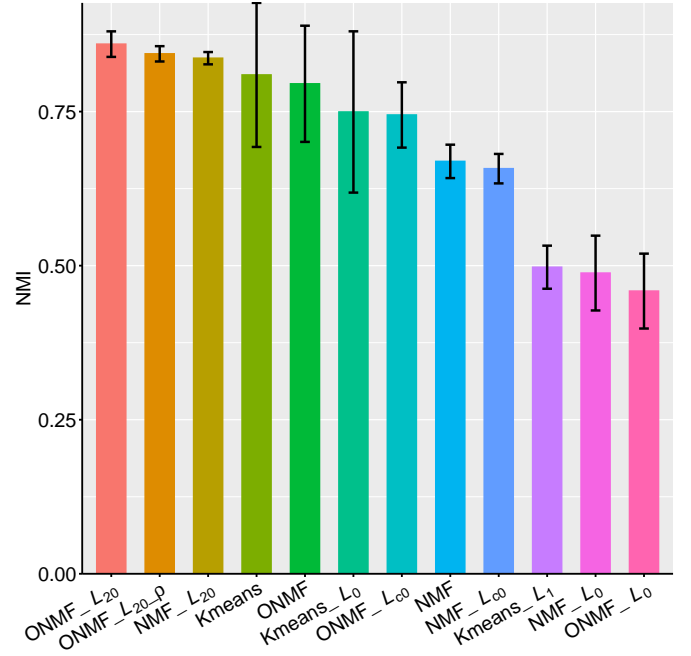


Figure 3. Comparison of 12 unsupervised clustering methods in terms of NMI on the synthetic data. Note that we set  $\rho = 1$  for ONMF- $\ell_{20-\rho}$ .

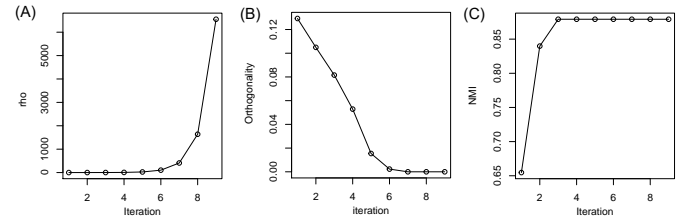


Figure 4. Scatter plots showing the change of (A)  $\rho$  in Algorithm 3, (B) orthogonality score of estimated  $\mathbf{H}$  and (C) NMI score. For the definition of orthogonality level, please see Eq. 23 of [25].

$\mathbf{X}$  satisfy  $X_{ij} \sim N(0, 1)$  ( $1 \leq i \leq 60, 1 \leq j \leq 20$ ),  $X_{ij} \sim N(0, 1)$  ( $31 \leq i \leq 90, 21 \leq j \leq 40$ ), and  $X_{ij} \sim 0.9 * N(0, 1)$  for other  $i$  and  $j$ . Secondly, we set  $X_{ij} := |X_{ij}|$  and obtain the final synthetic data. Note that the columns from 41 to 60 in  $\mathbf{X}$  correspond to outliers. We apply ONMF- $\ell_{20}$  with parameter  $k = 90$  to the synthetic data. We find that the outliers (*i.e.*, noise samples) are those with relatively small values in the estimated  $\mathbf{H}$  (Figure 5). This result implies ONMF- $\ell_{20}$  can detect these outliers by checking the values of columns in the estimated  $\mathbf{H}$ .

### C. Application to biological data

In this study, the proposed methods and other comparison methods are evaluated on three scRNA-seq datasets as follows:

- **Pollen** dataset [36] contains 301 single cells from 11 cell populations which are divided into 4 classes including Blood cells, Neural cells, Dermal or epidermal cells and Pluripotent cells.

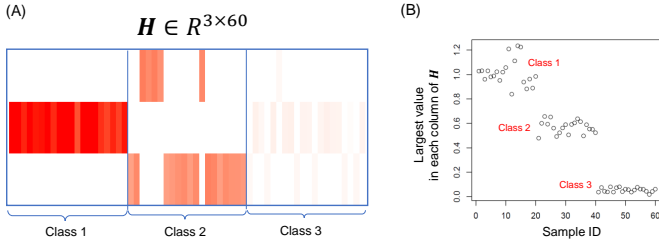


Figure 5. (A) Heatmap corresponding to the estimated  $H$  by ONMF- $\ell_{20}$  on the second synthetic data. (B) Scatter plot showing the largest values from each column of the estimated  $H$ .

- **Camp1** dataset [37] contains 425 single cells from human liver cells which are divided into 5 populations, named as iPS\_day\_0, De\_day\_6, IH\_day\_14, MH\_day\_21, and HE\_day\_8.
- **Lake** dataset [38] contains 3042 single cells from human liver cells which are divided into 16 populations named as Ex1, Ex3, Ex4, In6, In1, Ex5, In5, Ex7, In8, Ex2, Ex6, In7, In4, Ex8, In3, In2.

For each scRNA-seq dataset, we first filter out these genes which are not expressed in more than 70% of cells. We then use a logarithmic transformation  $x = \log_2(x)$  to transform raw expression data. After preprocessing, 8747, 8058 and 5000 genes are retained for Pollen, Camp1 and Lake datasets, respectively.

Table II  
COMPARISON IN TERMS OF (NMI %  $\pm$  STD), (PURITY %  $\pm$  STD) AND (ENTROPY %  $\pm$  STD) ON THE POLLEN, LAKE AND CAMP1 DATASETS.

Pollen data	#gene	NMI $\pm$ sd	Purity $\pm$ sd	Entropy $\pm$ sd
NMF- $\ell_{20}$	2000	<b>85.87 <math>\pm</math> 1.29</b>	<b>91.86 <math>\pm</math> 0.23</b>	<b>19.10 <math>\pm</math> 0.97</b>
ONMF- $\ell_{20-\rho}$	2000	84.96 $\pm$ 0.86	91.69 $\pm$ 0.16	19.79 $\pm$ 0.61
ONMF- $\ell_{20}$	2000	80.71 $\pm$ 3.56	89.30 $\pm$ 2.76	24.34 $\pm$ 4.30
ONMF- $\ell_{c0}$	*	81.62 $\pm$ 0.32	90.73 $\pm$ 0.11	22.28 $\pm$ 0.22
ONMF- $\ell_0$	*	51.67 $\pm$ 4.58	67.08 $\pm$ 5.65	27.56 $\pm$ 1.92
NMF- $\ell_0$	*	54.46 $\pm$ 6.86	67.34 $\pm$ 5.78	24.97 $\pm$ 5.59
NMF- $\ell_{c0}$	*	81.45 $\pm$ 0.88	91.89 $\pm$ 0.17	21.28 $\pm$ 0.69
ONMF	all	83.70 $\pm$ 2.81	91.23 $\pm$ 2.52	20.52 $\pm$ 4.07
Kmeans	all	71.39 $\pm$ 7.89	82.52 $\pm$ 5.27	31.37 $\pm$ 5.17
Kmeans- $\ell_0$	2000	72.36 $\pm$ 7.30	81.40 $\pm$ 8.25	29.48 $\pm$ 7.92
Kmeans- $\ell_1$	2039	78.09 $\pm$ 9.60	88.54 $\pm$ 7.01	21.45 $\pm$ 5.43
Camp1 data	#gene	NMI $\pm$ sd	Purity $\pm$ sd	Entropy $\pm$ sd
NMF- $\ell_{20}$	2000	<b>89.94 <math>\pm</math> 1.30</b>	<b>96.07 <math>\pm</math> 0.39</b>	9.88 $\pm$ 0.88
ONMF- $\ell_{20-\rho}$	2000	89.32 $\pm$ 3.16	92.40 $\pm$ 8.13	10.96 $\pm$ 3.68
ONMF- $\ell_{20}$	2000	71.00 $\pm$ 9.25	72.12 $\pm$ 5.54	29.04 $\pm$ 6.15
ONMF- $\ell_{c0}$	*	47.31 $\pm$ 8.06	44.35 $\pm$ 5.13	10.25 $\pm$ 3.95
ONMF- $\ell_0$	*	18.57 $\pm$ 18.69	34.14 $\pm$ 7.56	<b>5.85 <math>\pm</math> 4.99</b>
NMF- $\ell_0$	*	12.41 $\pm$ 17.04	31.25 $\pm$ 6.72	5.94 $\pm$ 6.38
NMF- $\ell_{c0}$	*	85.54 $\pm$ 5.20	91.67 $\pm$ 2.74	17.27 $\pm$ 4.10
ONMF	all	78.98 $\pm$ 9.88	78.31 $\pm$ 9.89	23.19 $\pm$ 8.71
Kmeans	all	78.06 $\pm$ 1.18	79.72 $\pm$ 5.76	24.09 $\pm$ 4.16
Kmeans- $\ell_0$	2000	73.13 $\pm$ 5.36	71.62 $\pm$ 7.18	28.67 $\pm$ 4.58
Kmeans- $\ell_1$	2005	71.96 $\pm$ 1.32	79.11 $\pm$ 1.10	28.07 $\pm$ 1.33
Lake data	#gene	NMI $\pm$ sd	Purity $\pm$ sd	Entropy $\pm$ sd
NMF- $\ell_{20}$	2000	<b>72.43 <math>\pm</math> 2.15</b>	<b>76.73 <math>\pm</math> 2.25</b>	28.88 $\pm$ 2.86
ONMF- $\ell_{20}$	2000	57.19 $\pm$ 4.16	63.92 $\pm$ 4.30	42.67 $\pm$ 5.01
ONMF- $\ell_{20-\rho}$	2000	71.99 $\pm$ 2.19	76.23 $\pm$ 2.49	29.60 $\pm$ 2.60
ONMF- $\ell_{c0}$	*	10.23 $\pm$ 10.54	36.97 $\pm$ 2.42	8.33 $\pm$ 8.70
ONMF- $\ell_0$	*	0.92 $\pm$ 0.64	35.01 $\pm$ 0.21	<b>1.53 <math>\pm</math> 1.42</b>
NMF- $\ell_0$	*	17.08 $\pm$ 14.82	41.30 $\pm$ 6.59	11.05 $\pm$ 11.93
NMF- $\ell_{c0}$	*	66.35 $\pm$ 2.20	72.00 $\pm$ 1.95	34.61 $\pm$ 3.22
ONMF	all	61.44 $\pm$ 3.84	67.08 $\pm$ 4.00	40.20 $\pm$ 4.43
Kmeans	all	59.96 $\pm$ 1.31	68.43 $\pm$ 1.68	42.10 $\pm$ 1.59
Kmeans- $\ell_0$	2000	62.05 $\pm$ 2.67	68.93 $\pm$ 2.62	40.01 $\pm$ 2.91
Kmeans- $\ell_1$	2270	70.73 $\pm$ 1.34	77.62 $\pm$ 2.12	32.32 $\pm$ 1.28

For ONMF- $\ell_{20}$ , we set  $k = 2000$  (to extract 2000 genes) which is to ensure that the number of selected genes is about 2000 for further analysis of biological function; rank  $r$  equal to the number of true classes of scRNA-seq datasets (herein  $r = 4$  for the Pollen dataset,  $r = 5$  for the Camp1 dataset and  $r = 16$  for the Lake dataset);  $\rho = 0.1$  and  $\gamma = 1.5$  which are for updating next  $\rho := \gamma\rho$  (herein  $\rho$  is updated up to 10 times); and  $\epsilon = 1e - 3$  in Algorithm 3. For fairness of comparison, we ensure these estimated  $W$  of all sparse learning methods including NMF- $\ell_{20}$ , ONMF- $\ell_{c0}$ , NMF- $\ell_{c0}$ , ONMF- $\ell_0$ , NMF- $\ell_0$  and Kmeans- $\ell_0$  have the same sparsity level, and all methods are repeated 10 times using different initial points for comparison.

We evaluate the clustering performance of all methods in terms of NMI, Purity and Entropy. The detailed results on the pollen, camp1 and lake datasets are summarized in Table II. These results show that the proposed SSNMF methods, especially NMF- $\ell_{20}$ , outperform other methods. The use of  $\ell_{2,0}$ -norm enables some SSNMF methods to select some important features by checking the non-zero rows of  $W$ . Finally, we also discuss the influence of  $k$ -choice on the clustering performance for these proposed SSNMF with  $\ell_{2,0}$ -norm methods and the results show that the proposed NMF- $\ell_{20}$  outperforms Kmeans- $\ell_0$  in different situations (Table III).

Table III  
COMPARISON OF (NMI %) AVERAGES WITH DIFFERENT NUMBER OF GENES ON THE POLLEN, CAMP1 AND LAKE DATASETS.

Pollen data ( $k=$ )	500	1000	2000	3000	4000	5000
NMF- $\ell_{20}$	81.77	84.46	85.87	85.70	85.04	85.04
ONMF- $\ell_{20}$	69.36	73.06	80.71	84.27	84.65	84.34
ONMF- $\ell_{20-\rho}$	82.35	84.09	84.96	86.02	85.21	85.04
Kmeans- $\ell_0$	80.79	76.98	72.36	71.04	71.57	69.49
Camp1 data ( $k=$ )	500	1000	2000	3000	4000	5000
NMF- $\ell_{20}$	91.56	91.84	89.94	90.11	90.28	90.28
ONMF- $\ell_{20}$	62.57	63.93	71.00	72.54	77.34	80.77
ONMF- $\ell_{20-\rho}$	90.59	90.80	89.32	89.21	89.24	89.03
Kmeans- $\ell_0$	74.26	73.41	73.13	76.28	75.31	74.23
Lake data ( $k=$ )	500	1000	2000	3000	4000	5000
NMF- $\ell_{20}$	72.96	72.88	72.43	72.34	72.29	72.23
ONMF- $\ell_{20}$	52.94	55.67	57.19	58.64	59.95	61.44
ONMF- $\ell_{20-\rho}$	72.48	72.37	71.99	71.67	71.55	71.52
Kmeans- $\ell_0$	70.83	69.25	62.05	58.83	56.17	55.65

#### D. Biological analysis

In this section, we show that the SSNMF with  $\ell_{2,0}$ -norm methods can be used for the identification of subpopulation and gene selection for scRNA-seq data. Based on the experiment results in the previous section, the NMF- $\ell_{20}$  achieved the best performance. Therefore, we select the computing results from NMF- $\ell_{20}$  ( $k = 2000$ ) on Pollen and Camp1 datasets as an example for further biological analysis. Some of the significant gene and sample expression patterns can be identified based on the output  $W \in R^{p \times r}$  and  $H \in R^{r \times n}$  from NMF- $\ell_{20}$ .

To be simplify, a biological functional bicluster is defined as a gene subset with a sample subset (also as cell subset). For each pair of  $w_i$  (in  $W$ ) and  $h^i$  (in  $H$ ), a bicluster is extracted based on the following computational steps.

- Step 1: For the  $i$ -th column of  $W$  ( $w_i$ ), the higher numerical values, the more important the corresponding



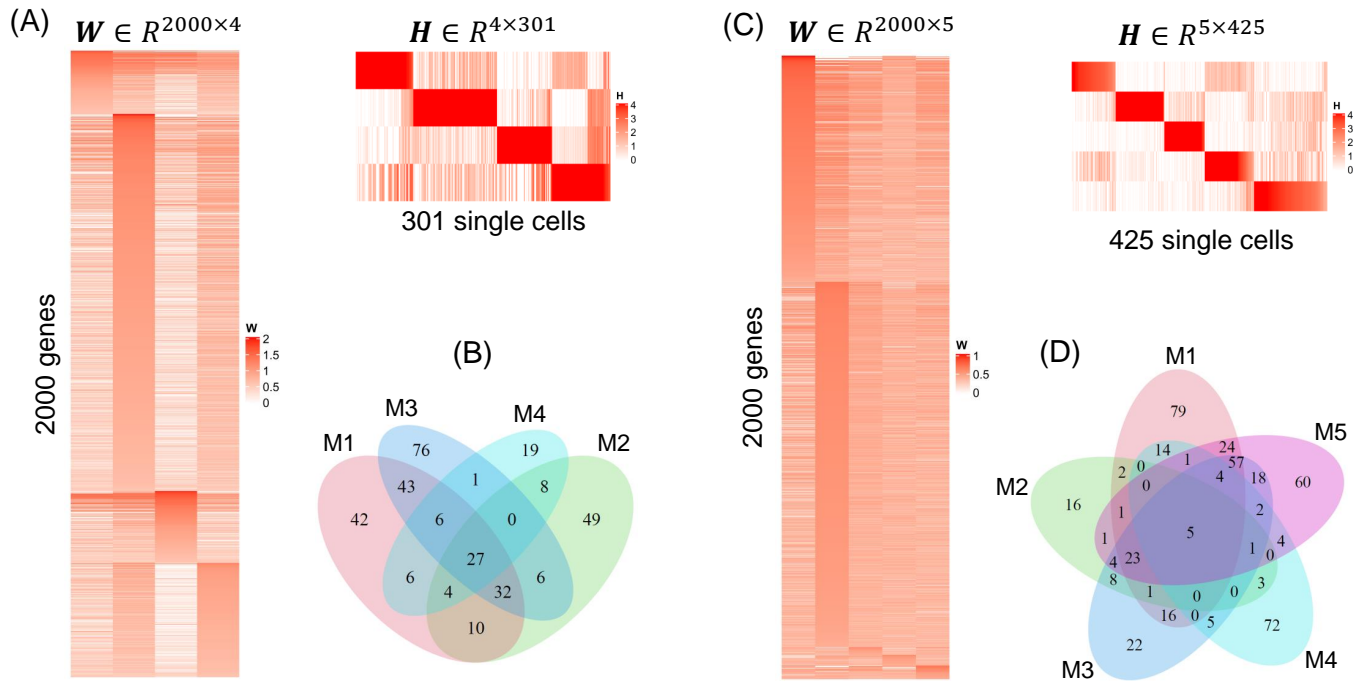


Figure 6. Results are shown in (A) to (D) when  $NMF_{\ell_{20}}$  is applied to the Pollen and Camp1 scRNA-seq datasets. (A) Heatmap showing  $W$  and  $H$  obtained from  $NMF_{\ell_{20}}$  with  $k = 2000$  on the Pollen dataset where 2000 genes are selected across 301 cells. (B) A Venn diagram showing overlap level for the selected genes from four biclusters (M1 to M4) on the Pollen dataset and total of 329 genes are selected. (C) Heatmap showing  $W$  and  $H$  obtained from  $NMF_{\ell_{20}}$  with  $k = 2000$  on the Camp1 dataset where 2000 genes are selected across 425 cells. (D) A Venn diagram showing overlap level for the selected genes from five biclusters (M1 to M5) on the Camp1 dataset and total of 443 genes are selected.

genes are. We do a z-score normalization for the  $w_i$  using the formula  $z_i = (w_i - \text{mean}(w_i)) / \text{sd}(w_i)$ . The genes with the corresponding coefficient values of  $w_i$ , whose z-scores are larger than a given threshold  $T$ , are extracted as the bicluster gene subset.

- Step 2: For  $i$ -th row of  $H$  ( $h^i$ ), we screen the cells with the largest coefficient in their corresponding column, i.e.,  $\{j | w_{ij} \geq w_{tj} \text{ for } j = 1, \dots, n, \forall t\}$ . Thus, we obtain a single cell set for the bicluster.

For the output  $W$  and  $H$  from Pollen dataset, we first calculate z-scores normalization for each column of  $W$  and then rank all genes according to their z-score values. These genes with z-score more than the threshold  $T = 1.5$  are regarded as the gene set of biclusters. We extract four biclusters with total 329 genes (Figure 6A and B). Bicluster 1 contains 170 genes and 68 cells. The selected cells are all Blood cells. Bicluster 2 contains 136 genes and 99 cells and all selected cells are Dermal/Epidermal cells. Bicluster 3 contains 191 genes and 65 cells and all selected cells are Neural cells. Bicluster 4 contains 71 genes and 69 cells while 45 of 69 cells are Blood cells and 24 of 69 are Pluripotent cells. To be interesting, some genes are shared in multiple biclusters. 27 genes are shared on all four biclusters. It shows that the genes may be hub genes and play a joint role in multiple biological functions (pathways).

To demonstrate the biological function of the gene sets from these identified biclusters, we perform the gene function enrichment analysis. We retrieve the KEGG pathways data information from Molecular Signatures Database (MSigDB,

<http://www.gsea-msigdb.org/gsea/msigdb/index.jsp>). KEGG pathways are a class of collection of manually drawn pathway maps representing the biological knowledge of the molecular interaction, reaction and relation networks. Each KEGG pathway is consisted by a set of functionally gene set which expresses complex regulatory mechanism among different genes. The hypergeometric test is applied for the biological statistical analysis. A class of critical KEGG signaling pathway is significantly enriched for the identified four bicluster gene sets with the Benjamini-Hochberg adjusted  $p < 0.05$ .

As expected, most of the enriched KEGG signaling pathways are related on the developing cerebral cortex which is highly consistent to the Pollen dataset from the diverse neural cell types [36]. Interestingly, we find that multiple bicluster gene sets are enriched on the ribosome pathway which is the cell factories responsible for making proteins and the ribosome pathway has been reported to play an important role in brain development [39]. In addition, some brain disease-related pathways have been discovered. For example, bicluster 1 is enriched in the pathways like Parkinson's disease ( $p = 7.5e-14$ ) and Alzheimer's disease ( $p = 3.9e-11$ ). Bicluster 2 is enriched in some KEGG pathways like proteasome ( $p = 1.2e-3$ ), leukocyte transendothelial migration ( $p = 1.2e-3$ ), regulation of actin cytoskeleton ( $p = 1.2e-3$ ), and focal adhesion ( $p = 1.4e-3$ ).

For the Camp1 dataset, five biclusters are extracted from the  $W$  and  $H$  (Figure 6C and D). Similarly, we calculate z-scores normalization for each column of  $W$  and then rank

all genes according to their z-score values. These genes with z-score more than the threshold  $T = 1.2$  are regarded as the gene set of biclusters. Bicluster 1 contains 227 genes and 73 cells where all selected cells are MH day 21 cells, bicluster 2 contains 65 genes and 81 cells where 80 of 81 cells are iPS day 0 cells, bicluster 3 contains 166 genes and 67 cells where all selected cells are De day 6 cells, bicluster 4 contains 111 genes and 82 cells where 77 of 82 cells are IH day 14 cells and 5 of 82 are MH day 21 cells, and bicluster 5 contains 205 genes and 122 cells where 113 of 122 cells are HE day 8 cells, 3 of 122 are De day 6 cells, 4 of 122 are IH day 14 cells and 2 of 122 are MH day 21 cells. Similar to the results on Pollen dataset, the cells in each identified bicluster are highly pure of population. Meanwhile, each bicluster possesses different domain genes while a small number of genes overlap each other (see Figure 6D). Due to these extracted single cells in the Camp1 dataset are from human liver [37], the biological function analysis show that the identified bicluster gene sets are significantly enriched a series of KEGG pathways (Benjamini-Hochberg adjusted  $p < 0.05$ ) which are highly related to biological processes associated with liver. For example, bicluster 1 is significantly enriched in the oxidative phosphorylation pathway ( $p = 7.6e - 13$  and there are 26 genes in this pathway) which have been reported to be related to liver [40]. Bicluster 2 is significantly enriched in the glycolysis gluconeogenesis pathway ( $p = 6.2e - 5$  and there are 6 genes in this pathway) which have been reported to be related to liver [41]. All these results show that the proposed method can be used for single cell type discovery, gene selection and biological process analysis.

## VI. CONCLUSION

In this paper, we present a class of SSNMF models with  $\ell_{2,0}$ -norm constraint. We prove that  $\ell_{2,0}$ -norm satisfies the KL property, such that the PALM algorithm can be used to solve a class of non-convex and non-smooth optimization problems with  $\ell_{2,0}$ -norm constraint. Especially, we first introduce the NMF- $\ell_{20}$  model which integrates feature selection in the NMF model. To improve the convergence rate of PALM, we further develop an accelerated version of PALM (maPALM) to solve NMF- $\ell_{20}$ . We also prove the convergence of proposed algorithms (PALM and maPALM) when they are used to solve NMF- $\ell_{20}$ . To integrate feature selection and non-negative orthogonal constraint in the NMF model, we furthermore introduce the ONMF- $\ell_{20}$  model. We develop an efficient algorithm to solve it by using a penalty function method. Briefly, the algorithm converts ONMF- $\ell_{20}$  into a series of constrained and penalized NMF problems which can be solved by the PALM and maPALM algorithms. Finally, we compare these proposed SSNMF methods with other methods for clustering task on the synthetic and scRNA-seq data. The results show that the proposed SSNMF methods can be used not only for clustering (single cell type discovery), but also for gene selection and biological function analysis.

## APPENDIX A DEFINITIONS AND PROOFS

### A. Mathematical definitions for non-convex analysis

We introduce some mathematical definitions which are used in this study for non-convex analysis [22, 42, 43].

**Definition 5.** (Proper)  $f(\mathbf{x})$  is proper if  $\mathbf{dom}(f) := \{\mathbf{x} \in \mathbb{R}^n : f(\mathbf{x}) < +\infty\}$  is nonempty and  $f(\mathbf{x}) > -\infty$ .

**Definition 6.** (Lower semi-continuous)  $f(\mathbf{x})$  is lower semi-continuous if  $\liminf_{\mathbf{x} \rightarrow \mathbf{x}_0} f(\mathbf{x}) \geq f(\mathbf{x}_0)$  at any point  $\mathbf{x}_0 \in \mathbf{dom}(f)$ .

**Definition 7.** (Coercive Function)  $f(\mathbf{x})$  is called coercive if  $f(\mathbf{x})$  is bounded from below and  $f(\mathbf{x}) \rightarrow \infty$  if  $\|\mathbf{x}\| \rightarrow \infty$ .

**Definition 8.** (Lipschitz smooth)  $f(\mathbf{x})$  is Lipschitz smooth if it is differentiable and there exists  $L > 0$  and such that

$$\|\nabla f(\mathbf{x}) - \nabla f(\mathbf{y})\| \leq L\|\mathbf{x} - \mathbf{y}\|, \forall \mathbf{x}, \mathbf{y} \in \mathbb{R}^n.$$

Any such  $L$  is considered to as a Lipschitz constant for  $f(\mathbf{x})$ .

**Definition 9.** (Subdifferential) Let  $f : \mathbb{R}^n \rightarrow (-\infty, \infty]$  be a proper and lower semi-continuous function. Then the Frecht sub-differential of  $f$ , denoted as  $\hat{\partial}f$ , at point  $\mathbf{x} \in \mathbf{dom}(f)$  is the set of all vectors  $\mathbf{z}$  which satisfies

$$\liminf_{\mathbf{x} \neq \mathbf{y}, \mathbf{y} \rightarrow \mathbf{x}} \frac{f(\mathbf{y}) - f(\mathbf{x}) - \langle \mathbf{z}, \mathbf{y} - \mathbf{x} \rangle}{\|\mathbf{y} - \mathbf{x}\|} \geq 0,$$

where  $\langle \cdot, \cdot \rangle$  denotes the inner product. Then the limiting Frecht sub-differential, or simply the sub-differential, denoted as  $\partial f$ , at  $\mathbf{x} \in \mathbf{dom}(f)$  is the following closure of  $\hat{\partial}f$ :

$$\{\mathbf{z} \in \mathbb{R}^n : \exists (\mathbf{x}^k, g(\mathbf{x}^k)) \rightarrow (\mathbf{x}, f(\mathbf{x}))\},$$

where  $\mathbf{z}^k \in \hat{\partial}f(\mathbf{x}^k) \rightarrow \mathbf{z}$  when  $k \rightarrow \infty$ .

**Definition 10.** (Critical Point) A point  $\mathbf{x}$  is called a critical point of function  $f$  if  $0 \in \partial f(\mathbf{x})$ .

**Definition 11.** (Semi-algebraic set and function) A subset  $\Omega$  of  $\mathbb{R}^n$  is a real semi-algebraic set if there exist a finite number of real polynomial functions  $r_{ij}, h_{ij} : \mathbb{R}^n \rightarrow \mathbb{R}$  such that

$$\Omega = \bigcup_{j=1}^p \bigcap_{i=1}^q \{\mathbf{x} \in \mathbb{R}^n : r_{ij}(\mathbf{x}) = 0 \text{ and } h_{ij}(\mathbf{x}) < 0\}.$$

Function  $f$  is called semi-algebraic function if its graph  $\{(\mathbf{x}, z) \in \mathbb{R}^{n+1} : f(\mathbf{x}) = z\}$  is a semi-algebraic subset of  $\mathbb{R}^{n+1}$ .

**Definition 12.** (Kurdyka-Łojasiewicz property and function) Function  $f$  has the Kurdyka-Łojasiewicz (KL) property at  $\bar{\mathbf{x}} \in \mathbf{dom}(\partial f) := \{\mathbf{x} \in \mathbb{R}^n : \partial f(\mathbf{x}) \neq \emptyset\}$  if there exist  $\eta \in (0, \infty]$ , a neighborhood  $U$  of  $\bar{\mathbf{x}}$  and a function  $\phi : [0, \eta] \rightarrow \mathbb{R}_+$  which satisfies (1)  $\phi$  is continuous at 0 and  $\phi(0) = 0$ ; (2)  $\phi$  is concave and  $C^1$  on  $(0, \eta)$ ; (3) for all  $s \in (0, \eta) : \phi'(s) > 0$ , such that for all  $\mathbf{x} \in U \cap [f(\bar{\mathbf{x}}) < f(\mathbf{x}) < f(\bar{\mathbf{x}}) + \eta]$ , the following inequality holds

$$\phi'(f(\mathbf{x}) - f(\bar{\mathbf{x}})) \text{dist}(0, \partial f(\mathbf{x})) \geq 1.$$

Function  $f$  is called a KL function if  $f$  satisfies the KL property at each point of  $\mathbf{dom}(\partial f)$ . Moreover, Theorem 3 in

[22] shows that all proper, lower semicontinuous and semi-algebraic functions satisfy KL property property.

### B. Proof of Proposition 1

*Proof.* Reference [25], we give the following proof. Let  $F_\rho(\mathbf{W}, \mathbf{H}) = \frac{1}{2}\|\mathbf{X} - \mathbf{W}\mathbf{H}\|_F^2 + \frac{\rho}{2}\sum_{j=1}^n \left( (\mathbf{1}^T \mathbf{h}_j)^2 - \|\mathbf{h}_j\|_2^2 \right)$ ,  $\mathbf{Z}^* := (\mathbf{W}^*, \mathbf{H}^*)$  is a local minimizer of (10). If  $\Omega_1$  is the feasible set of (7), then there exist a neighborhood of  $\mathbf{Z}^*$ ,  $N_\epsilon(\mathbf{Z}^*) = \{\mathbf{Z} \mid \|\mathbf{Z} - \mathbf{Z}^*\| \leq \epsilon\}$  where  $\epsilon > 0$  and it satisfies  $F_\rho(\mathbf{Z}^*) \leq F_\rho(\mathbf{Z})$  for any  $\mathbf{Z} \in N_\epsilon(\mathbf{Z}^*) \cap \Omega$ . Let  $\phi(\mathbf{h}_j) = (\mathbf{1}^T \mathbf{h}_j)^2 - \|\mathbf{h}_j\|_2^2$ , we note that  $\phi(\mathbf{h}_j) > 0$  if  $\mathbf{h}_j$  has at least two non-zeros entries and  $\phi(\alpha \mathbf{h}_j)$  is an increasing function with respect to  $\alpha$ . Suppose that there exists an  $j'$  and  $\mathbf{h}_{j'}$  is infeasible to (7) and thus  $\phi(\mathbf{h}_{j'}) > 0$ . Then, for a scalar  $\alpha \in (0, 1)$  and  $\mathbf{Z}_\alpha := (\mathbf{W}^*/\alpha, \alpha \mathbf{H}^*)$  is a feasible point to (10). Specifically, since  $\|\mathbf{Z}_\alpha - \mathbf{Z}^*\| = (1/\alpha - 1)^2 \|\mathbf{W}^*\|_F^2 + (\alpha - 1)^2 \|\mathbf{H}^*\|_F^2 \leq \max\{(1/\alpha - 1)^2, (\alpha - 1)^2\} \|\mathbf{Z}^*\|_F^2$ . To have  $\mathbf{Z}_\alpha \in N_\epsilon(\mathbf{Z}^*)$ , it is sufficient to let  $\max\{(1/\beta - 1)^2, (\beta - 1)^2\} < \alpha < 1$  where  $\beta = \sqrt{\epsilon/(2 * \|\mathbf{Z}^*\|_F^2)}$ . Thus, we have  $F_\rho(\mathbf{Z}_\alpha) - F_\rho(\mathbf{Z}^*) = \phi(\alpha \mathbf{h}_{j'}) - \phi(\mathbf{h}_{j'}) < 0$ . This is a contradiction. So, we have proved that  $(\mathbf{W}^*, \mathbf{H}^*)$  is a feasible solution of (7). Next, will prove that  $(\mathbf{W}^*, \mathbf{H}^*)$  is also a local minimizer of (7). Let  $\Omega_2$  as the feasible set of (7), then we have  $\{N_\epsilon(\mathbf{Z}^*) \cap \Omega_2\} \subseteq \{N_\epsilon(\mathbf{Z}^*) \cap \Omega_1\}$ . This implies that  $G_\rho(\mathbf{Z}^*) = F_\rho(\mathbf{Z}^*) \leq F_\rho(\mathbf{Z}) = G_\rho(\mathbf{Z})$  for any  $\mathbf{Z} \in N_\epsilon(\mathbf{Z}^*) \cap \Omega_2$  where  $G_\rho(\mathbf{W}, \mathbf{H}) = \frac{1}{2}\|\mathbf{X} - \mathbf{W}\mathbf{H}\|_F^2$ . So, we prove that  $(\mathbf{W}^*, \mathbf{H}^*)$  is a local minimizer of (7).  $\square$

### ACKNOWLEDGMENT

This work was supported by Key-Area Research and Development Program of Guangdong Province [2020B0101350001], and the National Science Foundation of China [61272274], and Natural Science Foundation of Jiangxi Province of China [20192BAB217004] and China Postdoctoral Science Foundation [2020M671902].

### REFERENCES

- [1] M. D. Luecken and F. J. Theis, "Current best practices in single-cell ma-seq analysis: a tutorial," *Mol. Syst. Biol.*, vol. 15, no. 6, p. e8746, 2019.
- [2] V. Y. Kiselev, T. S. Andrews, and M. Hemberg, "Challenges in unsupervised clustering of single-cell RNA-seq data," *Nat. Rev. Genet.*, vol. 20, no. 5, pp. 273–282, 2019.
- [3] J.-P. Brunet, P. Tamayo, T. R. Golub, and J. P. Mesirov, "Metagenes and molecular pattern discovery using matrix factorization," *Proc. Natl. Acad. Sci.*, vol. 101, no. 12, pp. 4164–4169, 2004.
- [4] M. Stražar, M. Žitnik, B. Zupan, J. Ule, and T. Curk, "Orthogonal matrix factorization enables integrative analysis of multiple ma binding proteins," *Bioinformatics*, vol. 32, no. 10, pp. 1527–1535, 2016.
- [5] J.-X. Liu, D. Wang, Y.-L. Gao, C.-H. Zheng, Y. Xu, and J. Yu, "Regularized non-negative matrix factorization for identifying differentially expressed genes and clustering samples: a survey," *IEEE/ACM Trans. Comput. Biol. Bioinform.*, vol. 15, no. 3, pp. 974–987, 2017.
- [6] S. Zhang, C.-C. Liu, W. Li, H. Shen, P. W. Laird, and X. J. Zhou, "Discovery of multi-dimensional modules by integrative analysis of cancer genomic data," *Nucleic Acids Res.*, vol. 40, no. 19, pp. 9379–9391, 2012.
- [7] J. Chen and S. Zhang, "Discovery of two-level modular organization from matched genomic data via joint matrix trifactorization," *Nucleic Acids Res.*, vol. 46, no. 12, pp. 5967–5976, 2018.
- [8] L. Zhang and S. Zhang, "Learning common and specific patterns from data of multiple interrelated biological scenarios with matrix factorization," *Nucleic Acids Res.*, vol. 47, no. 13, pp. 6606–6617, 2019.
- [9] X. Fu, K. Huang, N. D. Sidiropoulos, and W.-K. Ma, "Nonnegative matrix factorization for signal and data analytics: Identifiability, algorithms, and applications," *IEEE Signal Process. Mag.*, vol. 36, no. 2, pp. 59–80, 2019.
- [10] C. Shao and T. Höfer, "Robust classification of single-cell transcriptome data by nonnegative matrix factorization," *Bioinformatics*, vol. 33, no. 2, pp. 235–242, 2017.
- [11] Z. Duren, X. Chen, M. Zamanighomi, W. Zeng, A. T. Satpathy, H. Y. Chang, Y. Wang, and W. H. Wong, "Integrative analysis of single-cell genomics data by coupled nonnegative matrix factorizations," *Proc. Natl. Acad. Sci.*, vol. 115, no. 30, pp. 7723–7728, 2018.
- [12] J. D. Welch, V. Kozareva, A. Ferreira, C. Vanderburg, C. Martin, and E. Z. Macosko, "Single-cell multi-omic integration compares and contrasts features of brain cell identity," *Cell*, vol. 177, no. 7, pp. 1873–1887, 2019.
- [13] P. O. Hoyer, "Non-negative matrix factorization with sparseness constraints," *J. Mach. Learn. Res.*, vol. 5, no. Nov, pp. 1457–1469, 2004.
- [14] H. Kim and H. Park, "Sparse non-negative matrix factorizations via alternating non-negativity-constrained least squares for microarray data analysis," *Bioinformatics*, vol. 23, no. 12, pp. 1495–1502, 2007.
- [15] R. Peharz and F. Pernkopf, "Sparse nonnegative matrix factorization with  $\ell_0$ -constraints," *Neurocomputing*, vol. 80, pp. 38–46, 2012.
- [16] J. Li, K. Cheng, S. Wang, F. Morstatter, R. P. Trevino, J. Tang, and H. Liu, "Feature selection: A data perspective," *ACM Comput. Surv.*, vol. 50, no. 6, pp. 1–45, 2017.
- [17] J. Gui, Z. Sun, S. Ji, D. Tao, and T. Tan, "Feature selection based on structured sparsity: A comprehensive study," *IEEE Trans. Neural Netw. Learn. Syst.*, vol. 28, no. 7, pp. 1490–1507, 2017.
- [18] F. Nie, H. Huang, X. Cai, and C. H. Ding, "Efficient and robust feature selection via joint  $\ell_{21}$ -norms minimization," in *Adv. Neural. Inf. Process. Syst.*, 2010, pp. 1813–1821.
- [19] H. Huang, C. Ding, and D. Luo, "Towards structural sparsity: An explicit  $\ell_2/\ell_0$  approach," in *IEEE 10th Int. Conf. Data Mining*, 2010, pp. 344–353.
- [20] T. Pang, F. Nie, J. Han, and X. Li, "Efficient feature selection via  $\ell_{2,0}$ -norm constrained sparse regression," *IEEE Trans. Knowl. Data Eng.*, vol. 31, no. 5, pp. 880–893, 2019.
- [21] X. Du, F. Nie, W. Wang, Y. Yang, and X. Zhou, "Exploiting combination effect for unsupervised feature selection by  $\ell_{20}$  norm," *IEEE Trans. Neural Netw. Learn. Syst.*, vol. 30, no. 1, pp. 201–214, 2018.
- [22] J. Bolte, S. Sabach, and M. Teboulle, "Proximal alternating linearized minimization for nonconvex and nonsmooth problems," *Math. Program.*, vol. 146, no. 1-2, pp. 459–494, 2014.
- [23] C. Ding, T. Li, W. Peng, and H. Park, "Orthogonal nonnegative matrix t-factorizations for clustering," in *Proc. 12th ACM Int. Conf. Knowl. Discovery Data Mining*, 2006, pp. 126–135.
- [24] K. Zhang, S. Zhang, J. Liu, J. Wang, and J. Zhang, "Greedy orthogonal pivoting algorithm for non-negative matrix factorization," in *Int. Conf. Mach. Learn.*, 2019, pp. 7493–7501.
- [25] S. Wang, T.-H. Chang, Y. Cui, and J.-S. Pang, "Clustering by orthogonal nmf model and non-convex penalty optimization," *arXiv preprint arXiv:1906.00570*, 2019.
- [26] D. D. Lee and H. S. Seung, "Learning the parts of objects by non-negative matrix factorization," *Nature*, vol. 401, no. 6755, pp. 788–791, 1999.
- [27] H. Li and Z. Lin, "Accelerated proximal gradient methods for nonconvex programming," in *Adv. Neural. Inf. Process. Syst.*, 2015, pp. 379–387.

- [28] Q. Li, Y. Zhou, Y. Liang, and P. K. Varshney, "Convergence analysis of proximal gradient with momentum for nonconvex optimization," in *Int. Conf. Mach. Learn.*, 2017, pp. 2111–2119.
- [29] Y. Xu and W. Yin, "A globally convergent algorithm for nonconvex optimization based on block coordinate update," *J. Sci. Comput.*, vol. 72, no. 2, pp. 700–734, 2017.
- [30] N. Guan, D. Tao, Z. Luo, and B. Yuan, "NeNMF: An optimal gradient method for nonnegative matrix factorization," *IEEE Trans. Signal Process.*, vol. 60, no. 6, pp. 2882–2898, 2012.
- [31] Y. Xu and W. Yin, "A block coordinate descent method for regularized multiconvex optimization with applications to non-negative tensor factorization and completion," *SIAM J. Imaging Sci.*, vol. 6, no. 3, pp. 1758–1789, 2013.
- [32] T. Pock and S. Sabach, "Inertial proximal alternating linearized minimization (iPALM) for nonconvex and nonsmooth problems," *SIAM J. Imaging Sci.*, vol. 9, no. 4, pp. 1756–1787, 2016.
- [33] D. M. Witten and R. Tibshirani, "A framework for feature selection in clustering," *J. Am. Stat. Assoc.*, vol. 105, no. 490, pp. 713–726, 2010.
- [34] X. Chang, Y. Wang, R. Li, and Z. Xu, "Sparse k-means with  $\ell_\infty/\ell_0$  penalty for high-dimensional data clustering," *Stat. Sin.*, vol. 28, no. 3, pp. 1265–1284, 2018.
- [35] Z. Li, J. Liu, Y. Yang, X. Zhou, and H. Lu, "Clustering-guided sparse structural learning for unsupervised feature selection," *IEEE Trans. Knowl. Data Eng.*, vol. 26, no. 9, pp. 2138–2150, 2014.
- [36] A. A. Pollen *et al.*, "Low-coverage single-cell mRNA sequencing reveals cellular heterogeneity and activated signaling pathways in developing cerebral cortex," *Nat. Biotechnol.*, vol. 32, no. 10, p. 1053, 2014.
- [37] J. G. Camp *et al.*, "Multilineage communication regulates human liver bud development from pluripotency," *Nature*, vol. 546, no. 7659, p. 533, 2017.
- [38] B. B. Lake, R. Ai, G. E. Kaeser *et al.*, "Neuronal subtypes and diversity revealed by single-nucleus RNA sequencing of the human brain," *Science*, vol. 352, no. 6293, pp. 1586–1590, 2016.
- [39] K. F. Chau, M. L. Shannon, R. M. Fame, E. Fonseca, H. Mullan, M. B. Johnson, A. K. Sendamarai, M. W. Springel, B. Laurent, and M. K. Lehtinen, "Downregulation of ribosome biogenesis during early forebrain development," *Elife*, vol. 7, p. e36998, 2018.
- [40] F. Santacatterina, L. Sánchez-Cenizo *et al.*, "Down-regulation of oxidative phosphorylation in the liver by expression of the atpase inhibitory factor 1 induces a tumor-promoter metabolic state," *Oncotarget*, vol. 7, no. 1, p. 490, 2016.
- [41] R. Ma, W. Zhang, K. Tang *et al.*, "Switch of glycolysis to gluconeogenesis by dexamethasone for treatment of hepatocarcinoma," *Nat. Commun.*, vol. 4, no. 1, pp. 1–12, 2013.
- [42] R. Liu, S. Cheng, Y. He, X. Fan, Z. Lin, and Z. Luo, "On the convergence of learning-based iterative methods for nonconvex inverse problems," *IEEE Trans. Pattern Anal. Mach. Intell.*, vol. 42, no. 12, pp. 3027–3039, 2020.
- [43] C. Bao, H. Ji, Y. Quan, and Z. Shen, "Dictionary learning for sparse coding: Algorithms and convergence analysis," *IEEE Trans. Pattern Anal. Mach. Intell.*, vol. 38, no. 7, pp. 1356–1369, 2015.